Reprinted with permission from the publisher.
In: IEEE Electron Device Letters 2004.
Vol. 25, No. 4, pp. 173–175.

Square-Extensional Mode Single-Crystal Silicon Micromechanical Resonator for Low-Phase-Noise Oscillator Applications

Ville Kaajakari, Tomi Mattila, *Member, IEEE*, Aarne Oja, Jyrki Kiihamäki, and Heikki Seppä

***Abstract*—A micromechanical 13.1-MHz bulk acoustic mode silicon resonator having a high quality factor ($Q = 130\,000$) and high maximum drive level ($P = 0.12$ mW at the hysteresis limit) is demonstrated. The prototype resonator is fabricated of single-crystal silicon by reactive ion etching of a silicon-on-insulator wafer. A demonstration oscillator based on the new resonator shows single-sideband phase noise of −138 dBc/Hz at 1 kHz offset from the carrier.**

***Index Terms*—Bulk acoustic wave devices, microresonators, oscillator noise, oscillators, phase noise, resonators, silicon-on-insulator (SOI) technology.**

I. Introduction

MODERN wireless applications are setting increasing demands for the oscillator size, power consumption, and price. The conventional quartz crystal-based low-phase-noise oscillators are typically centimeter sized and appear bulky in the otherwise highly integrated transceiver architectures. Micromechanical resonators offer a promise of compact size, low power consumption, and integrability with IC electronics, and are thus, a very attractive potential alternative for the quartz crystals [1].

A low-phase-noise oscillator requires a resonator capable of a high quality factor and a large power output [2], [3]. Both requirements are typically met using quartz crystals, in particular the large physical size of quartz resonators accommodates high drive levels. In contrast, as the resonator size is dramatically reduced in the case of microresonators, the low power capacity limits the achievable oscillator noise floor [4].

This letter describes a 13.1-MHz micromechanical resonator which, for the first time, provides oscillator phase noise performance typically required in wireless communication applications. The resonator is based on a two-dimensional (2-D) bulk acoustic vibration mode that allows a maximum drive level $P = 0.12$ mW and a quality factor $Q = 130\,000$.

II. Resonator Structure and Fabrication

Fig. 1 shows the schematic and scanning electron microscope (SEM) image of the resonator. The resonator size is $320 \times 320 \times 10$ μm. The surface orientation is (100) and the plate sides are aligned in the $\langle 110 \rangle$ crystal directions. The T-type corner anchoring is used for reducing the energy leakage to the substrate.

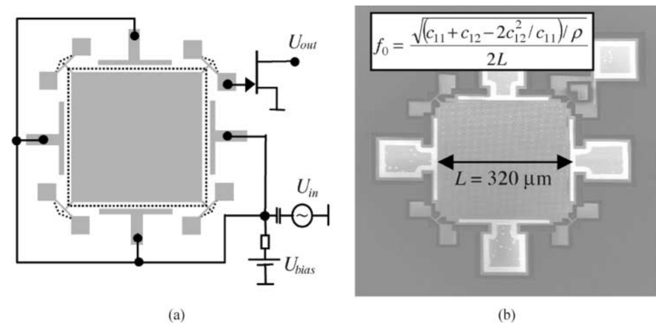

Fig. 1. Square-extensional microresonator ($f_0 = 13.1$ MHz and $Q = 130\,000$). (a) Schematic of the resonator showing the vibration mode in the expanded shape and biasing and driving setup. (b) SEM image of the resonator.

The component was made by deep reactive ion etching of silicon-on-insulator (SOI) wafer. For the hydrogen fluoride (HF) release, the plate was perforated with a 39×39 matrix of 1.5 μm diameter holes. The structural silicon layer and the substrate were heavily boron-doped ($\rho_B \approx 5 \cdot 10^{18}$ cm^{-3}) for electrical conductivity.

III. Resonator Model

As shown on the schematic in Fig. 1, the vibration mode can be characterized as a square plate zooming in and out thus preserving the original shape. This is in contrast with the well-known Lamé-mode in which the square edges bend in antiphase preserving the plate volume [5]. Our resonator also exhibits the Lamé-mode (at $f_0 = 12.1$ MHz, $Q = 60\,000$), but it is not excited in the symmetrical four-electrode configuration.

The mode can be approximated as a superposition of two orthogonal sound waves with the displacements given by $u_x = A \sin \pi x/L$ and $u_y = A \sin \pi y/L$, where A is the vibration amplitude, L is the plate size, and x and y indicate the position on the plate. This biaxial motion in x and y direction, with minimal rotation and shear, is a consequence of Poisson's ratio between the [110]- and [$\bar{1}$10]-direction being very small ($\nu = 0.06$). Thus, the square resonator shape, instead of circular [6], optimally accommodates the anisotropic elasticity of single-crystal silicon. The analytical mode shape was verified with a three–dimensional (3-D) finite element model (FEM) that included the silicon anisotropic elastic properties.

Manuscript received November 13, 2003. This work was supported in part by the Nokia Research Center, Okmetic, STMicroelectronics, VTI Technologies, and the Finnish National Technology Agency. The review of this letter was arranged by Editor J. Sin.

The authors are with VTT Information Technology, FIN-02044 Espoo, Finland.

Digital Object Identifier 10.1109/LED.2004.824840

© 2004 IEEE

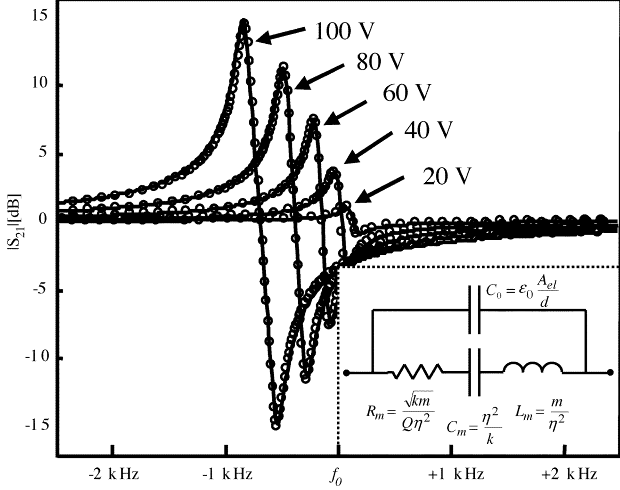

Fig. 2. (○) Measured and (−) simulated transmission response (f_0 = 13.1 MHz). Arrows indicate different bias voltages. Quality factor, gap spacing, and parasitic capacitance were adjusted for the best fit. Inset: electrical equivalent circuit.

By integrating the mode shape, a lumped one degree of freedom model shown in the inset of Fig. 2 is obtained. The circuit components depend on the effective spring constant k, the effective mass m, the quality factor Q, the electromechanical transduction factor $\eta = U_{\rm bias} C_0/d$, the electrode area $A_{\rm el}$, and the electrode gap d [4]. The effective mass and effective spring constant are related to the device geometry by

$$\begin{aligned} m &= \rho h L^2 \\ k &= \pi^2 Y_{\rm 2D} h \end{aligned} \tag{1}$$

where ρ is the silicon density, h is the device height, and $Y_{\rm 2D}$ is the effective elastic modulus for the 2-D expansion. For a plate without holes this is $Y_{\rm 2D} = c_{11} + c_{12} - 2c_{12}^2/c_{11} = 181$ GPa, where c_{11} and c_{12} are the silicon stiffnesses. The resonant frequencies obtained with the analytical approximation and FEM simulation agree within 0.5% for a solid plate confirming the validity of the model. The first-order lumped model has also been refined to include the effects of frequency shift due to bias voltage and capacitive and mechanical nonlinearity [7], [8].

IV. Measured Resonator Characteristics

The prototype resonator was measured using an HP4195A network analyzer and a JFET (Philips BF545B) preamplifier [4]. The resonator was dc-biased using 100-kΩ resistors. To minimize the parasitic capacitance, the resonator substrate was grounded and consequently the largest feed through path is the work capacitance C_0. Fig. 2 shows small-signal level ($u_{\rm ac}$ = 50 mV) transmission curves at different bias voltages showing a good agreement with the measured and simulated data. The mechanical resonance appears at $f_0 = 13.112$ MHz, which is about 4.7% lower than the result for a solid plate without the etch holes. With increasing bias voltage, the resonator peak shifts to a lower frequency due to the first-order nonlinearity in a parallel plate electromechanical coupling that results in electrical spring softening [4]. Based on the measured data, the mechanical unloaded quality factor is estimated to be $Q = 130\,000$. The other resonator characteristics are summarized in Table I.

TABLE I
Resonator Dimensions and Characteristic Parameters Measured at $U_{\rm bias} = 100$ V

Parameter	Symbol	Value	Units
Resonator side length	L	320	[μm]
Electrode length	L_{el}	290	[μm]
Resonator height	h	10	[μm]
Transducer gap	d_0	0.75	[μm]
Effective spring constant	k	16.2	[MN/m]
Effective mass	m	2.39	[nkg]
Quality factor	Q	130 000	
Motional capacitance	C_m	20.8	[aF]
Motional inductance	L_m	7.07	[H]
Motional resistance	R_m	4.47	[kΩ]

The resonator drive level, typically expressed as the power dissipated in the resonator, sets the oscillator noise floor and is directly proportional to stored mechanical energy ($P = \omega E/Q$) [2], [3]. For the demonstrated resonator, the energy storage was limited by mechanical nonlinearities, which caused hysteresis in the resonator transmission response at the vibration amplitude $x_{\rm vib}$ = 155 nm ($i_{\rm max}$ = 160 μA at $U_{\rm bias}$ = 100 V). This translates into maximum drive level $P = 0.12$ mW and stored energy $E = 190$ nJ. The high value arises from

1) the 2-D bulk acoustic vibration mode of the resonator that results in large effective mass and mechanical stiffness;
2) the high linearity of silicon as a mechanical material;
3) the high ratio of mechanical stiffness to nonlinear electrical coupling terms [7], [8].

Normalizing the stored energy with the resonator volume we obtain $E/V = 1.9 \cdot 10^5$ J/m^3. The corresponding typical hysteresis limit of AT-cut quartz crystal is only E/V = 500 J/m^3 [9]. Thus, the crucial observation is that silicon is capable of storing over two orders of magnitude higher mechanical energy densities than quartz. This partly compensates for the small size of the microresonators in their power handling capacity. It should be noted that the maximum power output is not limited by the dissipation-related self-heating effects that are not a dominant factor in the demonstrated resonator due to high thermal conductivity in silicon.

The rather high bias voltage is a direct consequence of the large 0.75-μm electrode gap used in the prototype. With an additional mask and fairly straightforward modification of the fabrication process, it is possible to fabricate 60-nm gaps [10]. The electromechanical transduction factor scales as $\eta \sim U_{\rm bias}/d_0^2$, and thus reducing the gap to 100 nm would allow a motional impedance of 64 Ω at 15-V bias voltage.

V. Oscillator Demonstration

Fig. 3 shows the noise-to-signal ratio for an oscillator based on a discrete amplifier circuit (Philips BF545B) connected in series feedback configuration with the square-extensional resonator inside a vacuum chamber ($p < 0.01$ mBar). The resonator bias voltage was $U_{\rm bias}$ = 75 V and the noise level of the dc-source was less than 1 μV/$\sqrt{\rm Hz}$. The vibration amplitude was limited to $x_{\rm vib}$ = 33 nm by the nonlinear gain characteristics of the amplifier circuit keeping the resonator in the

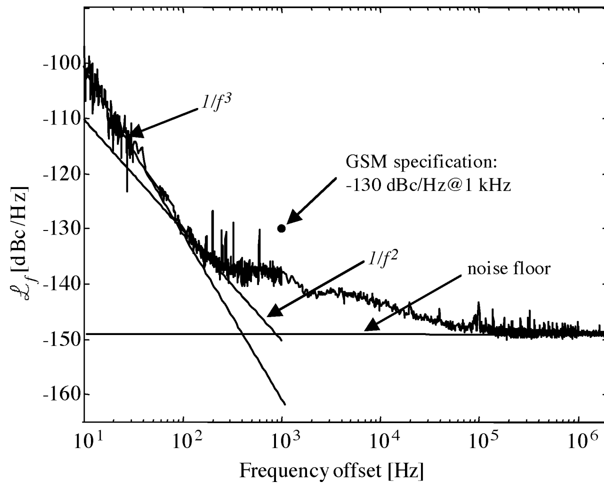

Fig. 3. Single-side band noise spectrum measured using Agilent series E5500 phase-noise measurement system. Spurious peaks have been removed. Resonant frequency is 13.1 MHz and drive level is 37 μA.

linear operation regime. To the authors' knowledge, the oscillator performance (-138 dBc/Hz at 1 kHz, noise floor -150 dBc/Hz) is the best reported for a MEMS based device and the first one to satisfy the GSM-specifications for the phase noise (typically -130 dBc/Hz at 1 kHz) typically achieved only with macroscale oscillators such as quartz crystals. Practical oscillator implementations utilize automatic gain control to limit the oscillation amplitude, which could further improve the phase noise performance.

VI. Conclusion

This letter demonstrates for the first time that in terms of phase noise, RF-MEMS can be a viable alternative to macroscale quartz resonators. Measured phase noise of -138 dBc/Hz at 1 kHz offset from the carrier is made possible by a new microresonator that offers high quality factor and high maximum drive level. For reference oscillator applications the temperature and long-term stability of the resonator will need to be addressed and these issues are under investigation.

Acknowledgment

The authors would like to thank V. Ermolov, H. Kuisma, M. de Labachelerie, and T. Ryhänen for useful discussions.

References

[1] C. T.-C. Nguyen, "Frequency-selective MEMS for miniaturized low-power communication devices," *IEEE Trans. Microwave Theory Tech.*, vol. 47, pp. 1486–1503, Aug. 1999.

[2] W.P. Robins, *Phase Noise in Signal Sources (Theory and Applications).* London, U.K.: Peter Peregrinus Ltd., 1982.

[3] T. Lee, *The Design of CMOS Radio-Frequency Integrated Circuits*. Cambridge, U.K.: Cambridge Univ. Press, 1998.

[4] T. Mattila, J. Kiihamäki, T. Lamminmäki, O. Jaakkola, P. Rantakari, A. Oja, H. Seppä, H. Kattelus, and I. Tittonen, "12 MHz micromechanical bulk acoustic mode oscillator," *Sens. Actuators A, Phys.*, vol. 1, no. 1, pp. 1–9, 2002.

[5] S. Basrour, H. Majjad, J. R. Coudevylle, and M. de Labachelerie, "Design and test of new high Q microresonators fabricated by UV-LIGA," *Proc. SPIE*, vol. 4408, pp. 310–316, Apr. 25–27, 2001.

[6] J. R. Clark, W.-T. Hsu, and C. T.-C. Nguyen, "High-Q VHF micromechanical contour-mode disk resonators," in *Proc. IEDM*, San Francisco, CA, Dec. 10–13, 2000, pp. 493–496.

[7] V. Kaajakari, T. Mattila, J. Kiihamäki, H. Kattelus, A. Oja, and H. Seppä, "Nonlinearities in single-crystal silicon micromechanical resonators," in *Proc. Transducers*, Boston, MA, June 9–12, 2003, pp. 1574–1577.

[8] T. Veijola and T. Mattila, "Modeling of nonlinear micromechanical resonators and their simulation with the harmonic-balance method," *Int. J. RF Microwave Comput. Aided Eng.*, vol. 11, no. 5, pp. 310–321, 2001.

[9] J. Nosek, "Drive level dependence of the resonant frequency in BAW quartz resonators and his modeling," *IEEE Trans. Ultrason., Ferroelect., Freq. Contr.*, vol. 46, pp. 823–829, Apr. 1999.

[10] E. Quévy, B. Legrand, D. Collard, and L. Buchaillot, "Ultimate technology for micromachining of nanometric gap HF micromechanical resonators," in *Proc. MEMS*, Kyoto, Japan, Jan. 19–23, 2003, pp. 157–160.